Materials and Devices
An International Scientific Journal
OPEN ACCESS
Freely Accessible Scientific Papers.
CA-IP
Managed by scientists for Science - http://co-ac.com

Conference paper (ISPDS2)

Raman-active modes in defective peapod

F. Fergani, S. M. Ait Abdelkader, H. Chadli, A. H. Rahmani, A. Rahmani

Laboratoire d'Etude des Matériaux Avancés et Applications (LEM2A), Université Moulay Ismail, Morocco.

Corresponding author : fati.fergani@gmail.com

RECEIVED: 17 january 2018 / RECEIVED IN FINAL FORM: 08 march 2018 / ACCEPTED: 09 march 2018

Abstract : The vibrational properties of defective single-walled carbon nanotube filled with C_{60} fullerene is the subject of the current study. For this aim we use the spectral moments method in the framework of the bond-polarization theory to calculate the nonresonant Raman spectra of hexa-vacancy defective C_{60} peapods. Essentially, the vibrational properties are closely coupled with the atomic structure of the system. The evolution of the Raman spectrum as a function of the spatial arrangement of defects in carbon nanotubes is discussed. This work provides benchmark theoretical results to understand the experimental data of defective C_{60} peapod.

Keywords : SINGLE WALL CARBON NANOTUBES, C_{60} PEAPODS, HEXA-VACANCY DEFECT, RAMAN SPECTROSCOPY, SPECTRAL MOMENT METHOD

Introduction

Since the pioneering study in 1998 by Smith et al.[1,2], single Wall carbon nanotubes (SWNT) filled with C_{60} fullerene molecules (called peapod) have attracting intensive interest in the material science and nanotechnology community on account of their interesting structure and their excellent electronical and mechanical properties. Thus, these materials represent a new class of hybrid systems between fullerenes and SWNTs where the encapsulated molecules (the peas) and the SWNT (the pod) are bonded through van der Waals interactions.

Using high-resolution transmission electron microscopy (HR-TEM), Suenaga and co-workers[3] elucidated that, the carbon nanotube is not perfect but it has a structural defects. There are several studies on the defects in SWNT structure and their effect on mechanical properties of SWNT[4,5], however only few literatures are available to date about the effect of defect in peapod. Experimentally peapod is made by a purification process, if this process is done imperfectly, some defects may remain on the wall of the peapod[6,7].

The evaluation of effects of defects and impurities on properties of these nanostructures would be crucial because of the inevitable creation of defects during the synthesis and purification processes[8] and under mechanical strains[9,10]. The most typical type of defects in crystalline lattices are point vacancies, interstitials, and bound complexes of the two. A missing or extra atom is a small perturbation in weakly bonded metal crystals, but it is not the same for the graphene. When vacancies and interstitials are highly disfavored, bond rotations are not, and these constitute the most prevalent type of defect in high quality graphites. A single bond rotation only affects four adjacent hexagons, converting two into pentagons and two into seven-sided heptagons, known in the literatura as a Stone-Wales (SW) defect.

The simplest defect type is a vacancy where a lattice site is unoccupied. The presence of vacancies may deteriorate the outstanding properties of nanotubes but may also have beneficial effects. In previous works of our group[11,12,13], we calculated the vibrational properties of non defect C_{60} peapods. In order to improve the comparison with the experimental Raman data measured on peapod samples, we calculate the nonresonant Raman spectra of C_{60} filled hexa-vacancy SWNT.

In this aim, we calculate the nonresonant Raman spectra in the framework of the bond-polarizability model combined with the spectral moment method.

This paper is organized in the following way. In Section 2 we present the used model and method. Results of calculations are the aim of Section 3, the final section is conclusions.

Model and method

Vacancy defects are always presented in SWNTs due to post-processing, including ion[14] and electron irradiation[15], and so on. In this study, we focus on vibrational properties of C_{60} inside hexa-vacancy defect in SWNT. The starting point for the majority simulation techniques is the calculation of the dynamical matrix of the system, and so will it be for this article. The dynamical matrix of C_{60} inside defective SWNT is calculated by block: the intramolecular interactions between carbon atoms at the surface of the C_{60} molecules are modelized by the force constants model described by Jishi and Dresselhaus[16], the C-C intratube interactions at the Surface of defective SWNT are calculated using Density Functional Theory (DFT) as implemented inside the SIESTA package[17] and the dynamical matrices associated with the coupling between the different subsystems (C_{60}-SWNT and C_{60}-C_{60} interactions) are described by the familiar (12-6) Lennard-Jones potential, $U_{LJ}(r) = 4\varepsilon\left[(\sigma/r)^{12} - (\sigma/r)^{6}\right]$, where r is the carbon atom-atom distance. We fixed $\varepsilon = 2.964$ meV and $\sigma = 0.3407$ nm according to Ref.[18].

Raman scattering studies has been extensively used to identify structural defect and nondefect in carbon nanotube and peapods. The intensities of the Raman lines are calculated within the empirical non-resonant bond polarizability model[19]. In this study we use the same bond polarizability parameters used in our previous work concerning the calculation of the Raman spectra of individual C_{60} and C_{70} peapods[12,20]. The D-band in the Raman spectra of sp^2 carbons is a signature of defects in the graphene lattice[21] and is often used to characterize defective SWNTs. However, the interpretation of the D-band feature might be ambiguous as a large observed D-band intensity might originate from one nanotube while the radial breathing mode (RBM) or graphitic G-band could be due to another tube present in the same sample[22].

Results

In this work, we focus primarily on vibrational properties of hexa-vacancy defect in both SWNT (see figure 1) and peapod. For this aim we study the Raman spectra of hexa-vacancy defect in (10,10) SWNT as a function of defect concentration. However, it is found from figure 2 that compared with that in the perfect SWNTs, although the hexa-vacancy leads to a redshift of the tube's RBM frequency. When the concentration of hexa-vacancies increases RBM downshift from 164 cm^{-1} in pristine tube to 161 cm^{-1}, 160 cm^{-1}, and 158 cm^{-1} for 2%, 3%, and 4% hexa-vacancies concentration in (10,10) SWNT, respectively. A second-lowest Raman-active mode located at 328 cm^{-1}, 330 cm^{-1}, 338 cm^{-1} for 2%, 3%, 4% hexa-vacancy concentrations for (10,10), this mode correspond to hexa-vacancy defect in (10,10) nanotube.

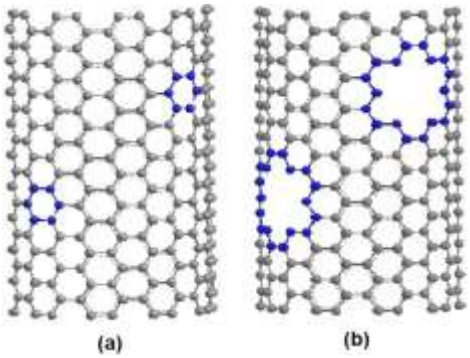

Figure 1: Schematic of both pristine (a) and hexa-vacancy defect (b) in SWNT.

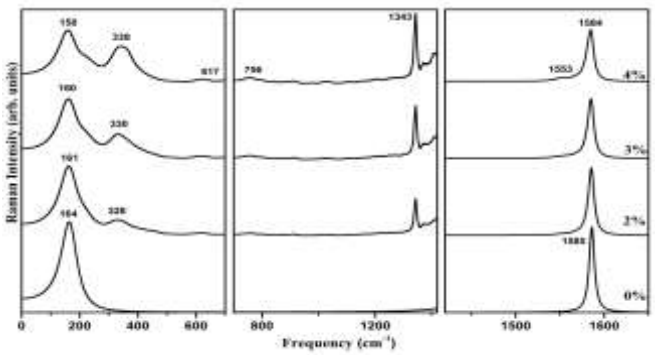

Figure 2: ZZ-polarized Raman spectra of armchair carbon nanotube (10,10) as a function of hexa-vacancies defects concentration.

The ratio of the D- to the G-band intensity (ID/IG), is usually used for a measurement of the disordered and the defect sites on carbon nanotubes walls, and it is useful to determine both the purity and the defect density, which has been difficult to accomplish by means other than Raman spectroscopy. In fact, the decrease of the intensity of the G mode upon defect creation increases the ID/IG intensity ratio, which could lead to an estimation of the amount of defects. The data in figure 3 shows the ID/IG ratio increased linearly for (10,10), from 0 to 10% concentration.

Because of their structural and vibrational properties, a lot of theoretical and experimental studies have been presented on C_{60} and C_{70} fullerenes and several interesting properties have been predicted or observed. Despite the large number of experimental results on the defect-induced changes to the Raman spectra of nanotubes samples the information that can be extracted from such analyses is limited and thus many issues remain unclear. In particular, the vibrational studies of defects peapods need more studies, for this purpose and in order to investigate the effect of hexa-vacancy defect on the oscillatory behavior of C_{60} peapod oscillators, we calculate ZZ-polarized Raman spectra of individual peapods for linear configuration of the C_{60} molecules inside (10,10) as a function of hexa-vacancy defect rates. For this purpose, four defect rates 0%, 0.6%, 1.2%, 1.8% in (10,10) have been considered, when the SWNTs fill with a 320, 269, 218, 167 C_{60}

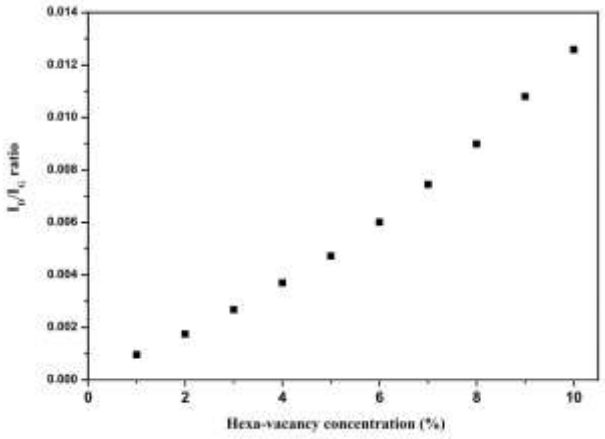

Figure 3: The intensity ratio ID/IG for (10,10) armchair SWNT is plotted as a function of the concentration of hexa-vacancy defect in the nanotube walls.

molecules, respectively, the results are shown in figure 4. The ZZ Raman spectra are displayed in the peapod radial breathing-like modes (PRBLM) range (left), in the region of the radial C_{60} modes and D band of defective SWNT (middle), and in the range of tangential modes: $A_g(2)$ mode of C_{60} and G-modes of the tubes (right).

The comparison between the calculated Raman spectra of perfect and defect peapods does not show significant differences in the intermediate and high-frequency regions except a new mode due to hexa-vacancy defect in SWNT (mode D) located at 1355 cm^{-1}. The modes located in the breathing-like mode range are very sensitive to the defect in SWNT because major changes in frequencies and intensities are observed. Concerning the RBLM mode of prestine C_{60}@(10,10) peapod is downshifted by 3 cm^{-1} independent of defect rate in peapod wall. Regarding the main lowest frequency Raman active modes of C_{60} no significant modification was observed in the $H_g(2)$ and $A_g(1)$ modes on defective peapod. By contrast, the increase of defect rate from 0% to 1,8% leads to a downshift of the $H_g(1)$ mode by 12 cm^{-1} with respect to the $H_g(1)$ mode of C_{60} molecule.

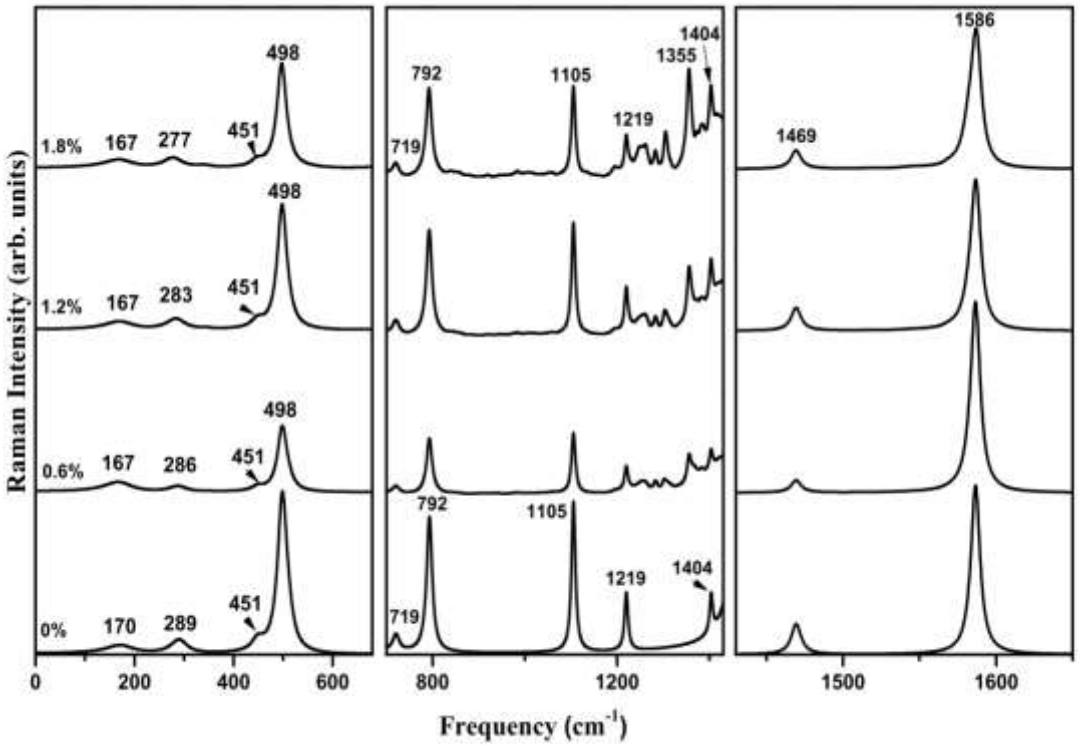

Figure 4: hexa-vacancy rate dependence of the ZZ-polarized Raman spectra of C_{60}@(10,10) peapods.

Conclusion

In this paper, we have studied defects of the polarized Raman spectra of hexa-vacancy in both (10,10) armchair single-walled carbon nanotube and C_{60}@(10,10) peapod as a function of the concentration of defects using the bond-polarizability model combined with the spectral moment's method. By examining the Raman intensities calculated for defective nanotube samples containing specific defects hexavacancy, we conclude that ID/IG ratios is sensitive to the defect concentration. All these predictions help us to explain the experimental Raman spectra of hexa-vacancy defect in nanotubes and in peapods.

Acknowledgements:

The work was supported by the CNRS-France/CNRST-Morocco agreement.

REFERENCES

1. B. W. Smith, M. Monthioux, D. E. Luzzi*, Nature,* **vol.396***,* p 323 (1998)
2. B. W. Smith, M. Monthioux, D. E. Luzzi, Chem. Phys. Lett*.,* **vol.315**, p 31 (1999)
3. K. Suenaga, T. Okazaki, K. Hirahara, S. Bandow, H. Kato, A. Taninaka, H. Shinohara, S. Iijima*, Appl. Phys. A,* **vol.76**, p 445 (2003)
4. X. Hao, H. Qiang, Y. Xiao-Hu, *Carbon,* **vol.45**, p 2486 (2007)
5. X. Hao, H. Qiang, Y. Xiao-Hu*, Compos. Sci. Technol,* **vol.68**, p 1809 (2008)
6. B.W. Smith, *Chem. Phys. Lett.,* **vol.321**, p 169174 (2000)
7. B. Burteaux, A. Claye, B.W. Smith, M. Monthioux, D.E. Luzzi, J.E. Fischer, *Chem. Phys. Lett.,* **vol.310**, p 21 (1999)
8. M. B. Nardelli, B. I. Yakobson, J. Bernholc, *Phys. Rev. B,* **vol.57**, p R4277 (1998)
9. W. Fa, F. Hu, J. Dong, *Phys. Lett. A,* **vol.331**, p 99 (2004)
10. H. Kim, J. Lee, S.-J. Kahng, Y.-W. Son, S.B. Lee, J. Ihm, Y. Kuk, *Phys. Rev. Lett.,* **vol.90**, p 216107 (2003)
11. H. Chadli, A. Rahmani, K. Sbai, J.-L. Sauvajol, *Physica A.,* **vol.358**, p 226 (2005)
12. F. Fergani, S. A. Abdelkader, H. Chadli, B. Fakrach, Ah. Rahmani, P. Hermet, and A. Rahmani, *Journal of Nanomaterials,* **vol.2017**, p 1 (2017)
13. H. Chadli, F. Fergani, S. A. Ait Abdelkader, AH Rahmani, B. Fakrach, A. Rahman, *Materials and Devices*, **vol.1, no. 1**, p 1221 (2016)
14. A. V. Krasheninnikov, K. Nordlund, M. Sirvi, E. Salonen, and J. Keinonen, *Phys. Rev. B,* **vol.63**, p 245405 (2001)
15. P. M. Ajayan, *Chem. Rev.*, **vol.99**, p 17871799 (1999)
16. R. A. Jishi, L. Venkataraman, M. S. Dresselhaus, G. Dresselhaus, *Chem. Phys. Lett.,* **vol.209**, p 77 (1993)
17. J. M. Soler, E. Artacho, J. D. Gale, A. Garca, J. Junquera, P. Ordejon, D. Sa nchez-Portal, *J. Phys.: Condens. Matter,* **vol.14**, p 2745 (2002)
18. H. Ulbricht, G. Moos, T. Hertel, *Phys. Rev. Lett.,* **vol.90**, p 095501 (2003).
19. S. Guha, J. Menendez, J.B. Page, G.B. Adams, *Phys. Rev. B,* **vol.53**, p 13106 (1996)
20. F. Fergani, H. Chadli, A. Belhboub, P. Hermet, A. Rahmani, *J. Phys. Chem. C,* **vol.119**, p 5679 (2015)
21. F. Tuinstra, J. L. Koenig, *J. Chem. Phys.,* **vol.53**, p 11261130 (1970)
22. W. A. Saidi, P. Norman, *Phys. Chem. Phys.,* **vol.16**, p 1479 (2014)